The VIRGO sensitivity curve

VIR-NOT-PER-1390-51

Author Name : Michele Punturo

Issue 7
Date : 21/7/2003

Introduction

The VIRGO sensitivity is limited by several noise source mechanisms. This note reports an updated list of the main noise contributions expected in VIRGO. The main reference for this note is the Virgo DAD [Ref: 1].

List of Constants

Here is a list of the parameter values employed to derive the individual contributions to the sensitivity curve (in IS units).

Physical Constants

Temperature	$T = 300K$
Boltzman constant	$k_b = 1.380658 \cdot 10^{-23}$
Plank constant	$h_p = 6.6260755 \cdot 10^{-34}$
Gravitational acceleration	$g = 9.8$
Light speed	$c = 3 \cdot 10^8$
Universal gravitational constant	$G = 6.670 \cdot 10^{-11}$
Earth radius	$R_E = 6370 \cdot 10^3$
Earth density	$\rho_E = 2 \cdot 10^3$

Material Constants

C85 steel (wires)

Density	$\rho_w = 7.9 \cdot 10^3$
Specific heat	$c_s = 502$
Specific heat / volume	$c_{st} = c_s \rho_w$
Thermal conductivity	$\kappa_{st} = 50$
Thermal expansion	$\alpha_{st} = 14 \cdot 10^{-6}$
Yield strength	$\sigma_B = 2.6 \cdot 10^9$
Youngs modulus	$E = 2.1 \cdot 10^{11}$

Fused Silica Mirrors

Density	$\rho_{FS} = 2.2 \cdot 10^3$
Specific heat	$c_{FS} = 682$
Specific heat / volume	$c_{FSt} = c_{FS} \rho_{FS}$
Thermal conductivity	$\kappa_{FS} = 2.1$
Thermal expansion	$\alpha_{FS} = 0.54 \cdot 10^{-6}$
Young Modulus	$E_{FS} = 7.36 \cdot 10^{10}$
Poisson Ratio	$\sigma_{FS} = 0.17$

Loss angles:

Far Mirrors (Herasil)	$\varphi_q = (0.711 \cdot 10^6)^{-1}$
Near Mirrors (Suprasil)	$\varphi_q = 1 \cdot 10^{-7}$

Vacuum Specifications

Tower Pressure	$P_T = 10^{-7}$
Pipe Pressure	$P_P = 10^{-5}$

Geometrical Parameters

Mirrors

Far Mirror height	$h_c = 0.096$
Input Mirror height	$h_c = 0.097$
Mirror radius	$R_c = 0.175$
Half wire spacing	$b_c = 0.025$
Mirror Mass	$m_c = \pi \cdot R_c^2 \cdot h_c \cdot \rho_{FS} = 21.166\ (20.320)$

Suspension Wires

Wire length	$L_w = 0.7$
Wire radius	$r_w = 100 \cdot 10^{-6}$

Laser & Interferometer Parameters

VIRGO arm length	$L_{arm} = 3000$
VIRGO pipe diameter	$D_{tube} = 1.2$
Horizontal-to-vertical coupling angle	$\theta_0 = L_{arm} /(2\ R_E)=2.35 \cdot 10^{-4}$
Effective (after the injection) Laser Power	$P_{las} = 10$
Finesse	$F = 50$
Laser wave length	$\lambda = 1.064 \cdot 10^{-6}$
Beam waist at the input mirror	$wN=2 \cdot 10^{-2}$
Beam waist at the end mirror	$wF=5.5 \cdot 10^{-2}$
Recycling factor	$C = 50$
Power at the beam splitter	$P_{bs}=P_{las} \cdot C=20 \cdot 50=1kW$
Power in the Fabry-Perot cavity	$P\text{cavity}=\frac{1}{2} P_{bs} \cdot (2F/\pi)=16kW$
Photodiode efficiency	$\eta = 0.85$

Noise Sources

Seismic Noise

The horizontal transfer function of each pendulum stage is given by:

$$\tilde{x}(w) = \frac{w_0^2 (1 + i j(w))}{\left(w_0^2 - w^2\right) + i w_0^2 j(w)} \cdot \tilde{x}_0(w) = \mathrm{T}(w) \cdot \tilde{x}_0(w)$$

[1]

where $\omega_0=(g/L_w)^{0.5}$. If $\omega \gg \omega_0$ and there are N attenuation stages, then

$$\tilde{x}(w) \approx \left(\frac{w_0^2}{w^2}\right)^{2N} \cdot \tilde{x}_{seism}(w)$$

[2]

The vertical attenuation is performed by the suspension blades in conjunction with the magnetic antisprings. The vertical residual seismic noise enters the interferometer signal because of the vertical-to-horizontal coupling due to the Earth curvature. The coupling angle is θ_0. All of the suspension chain has been simulated by A.Vicerè and we have used the resulting transfer function.
The seismic spectral amplitude adopted is given by:

$$\tilde{x}_{seim}(f) \approx \frac{A_0}{f^2}$$

[3]

with $A_0=10^{-7}$ for reference, but $A_0=10^{-6}$ has been used for comparison. The resulting equivalent h is

$$h_{seism}(f) = \frac{\sqrt{4}}{L_{arm}} \left\{HTF(f)^2 + \left[q_0 \cdot VTF(f)\right]^2\right\}^{\frac{1}{2}} \tilde{x}_{seim}(f)$$

[4]

where HTF(f) and VTF(f) are the horizontal and the vertical (simulated) S.A. transfer functions respectively.

Gravity Gradient Noise (Newtonian Noise)

The Newtonian noise is given by the static gravitational field modulation by the seismic noise. There are different models for the expected power spectrum [Ref: 2, Ref: 3]. We used the two different expressions to evaluate the different noise contribution.

$$h_{NN}^{[CC]}(f) \approx \frac{3 \cdot 10^{-11}}{f^2} \cdot \tilde{x}_{seim}(f)$$

[5]

$$h_{NN}^{[Thorne]}(f) = \sqrt{2}\, \frac{2.7 \cdot G \cdot r_E}{(2pf)^2 L_{arm}} \cdot \tilde{x}_{seim}(f)$$

[6]

Since the result is strongly model dependent and since it seems possible to subtract that noise from the interferometer signal, it has been decided to neglect the NN in the resulting sensitivity curve and to show the Cella-Cuoco (CC) model contribution superimposed on the sensitivity plot. The model [5] gives an amplitude larger by a factor of 7 with respect to [6].

Magnetic Noise

The seismic noise and the presence of magnets on the *marionetta* have an effect on the VIRGO sensitivity. There are essentially three processes [Ref: 1]:

- Diamagnetic marionetta-tower coupling:

$$\tilde{x}_{M1}(f) = \frac{1}{(2\pi f)^2 M_m} \cdot \frac{15\chi_{SS}\, \mu_0\, e_w\, m_\mu^2}{4\pi\, d_w^6} \tilde{x}_{seim}(f)$$

[7]

- Eddy currents on the tower walls:

$$\tilde{x}_{M2}(f) = \frac{1}{(2\pi f)^2 M_m} \cdot \frac{3\sqrt{2}\, \mu_0^2\, e_w\, m_\mu^2\, \sigma_{SS} \cdot f}{32\, d_w^4} \tilde{x}_{seim}(f)$$

[8]

- Marionetta fluctuation due to the eddy currents:

$$\tau_{diss} = \frac{64\pi\, d_w^4\, M_m}{3\mu_0^2\, e_w\, m_\mu^2\, \sigma_{SS}}$$

$$\tilde{x}_{M3}(f) = \frac{1}{(2\pi f)^2} \sqrt{\frac{8k_B T}{M_m \tau_{diss}}}$$

[9]

The equivalent h given by the "magnetic noise" is:

$$h_{Mag}(f) \approx \left|\mathrm{T}(2\pi f)\right| \cdot \frac{2}{L_{arm}} \cdot \sqrt{\tilde{x}_{M1}^2 + \tilde{x}_{M2}^2 + \tilde{x}_{M3}^2}$$

[10]

where T(ω) is given by EQ [1]. The constants used in the previous formulae are reported in Table 1:

Table 1

Parameter	Symbol	Value
Stainless Steel wall susceptibility	χ_{SS}	$5 \cdot 10^{-3}$
Marionetta Mass	M_m	100
Vacuum permettivity	μ_0	$4\pi \cdot 10^{-7}$
Magnet momentum	m_μ	0.12
Tower wall tickness	e_w	10^{-4}
Magnet-Wall distance	d_w	$3 \cdot 10^{-2}$
Stainless Steel conducibility	σ_{SS}	$1.4 \cdot 10^{6}$

Shot Noise

The shot noise expression can be obtained by [Ref: 4] or [Ref: 5]. If the noise level is calculated neglecting the modulation effect on the diode photocurrent, the formula is:

$$h_{Shot}(f) = \frac{1}{8 L_{arm} F} \cdot \sqrt{2h_p \frac{l\, c}{h\, C\, P_{las}}} \cdot \sqrt{1 + \left(\frac{f}{f_{FP}}\right)^2}$$

$$f_{FP} = \frac{c}{4 L_{arm} F}$$

[11]

If F=50 the Fabry-Perot cut-off frequency in VIRGO is $f_{FP} \approx 500$Hz. In this note the modulation effect has been taken in account (see F.Bondu, Ref 17) and a multiplication factor $(3/2)^{½}$must be put in the previous equation.

Radiation Pressure Noise

The expression for the radiation pressure noise can be obtained by [Ref: 4]. The formula is:

$$h_{rad}(f) = \frac{F}{m_c\, L_{arm}\, (p\, f)^2} \cdot \sqrt{\frac{\hbar}{2p} \frac{C\, P_{las}}{l\, c}}$$

[12]

Quantum Limit

The quantum limit pseudo-distribution is the collection of points where $h_{rad}=h_{Shot}$. The expression for that curve as function of the GW frequency is

$$h_{QL}(f) = \frac{1}{2p\, f \cdot L_{arm}} \cdot \sqrt{\frac{\hbar}{m_c} \cdot \sqrt{\frac{2}{h} \cdot \left[1 + \left(\frac{f}{f_{FP}}\right)^2\right]}}$$

[13]

Thermal noise

The thermal noise limit of the VIRGO sensitivity is due to the energy loss processes of the suspension wires and test masses.

Wire thermal noise

The suspension wires contribute to the thermal noise through 3 processes:

- Pendulum thermal oscillation
- Vertical thermal oscillation
- Violin modes

Pendulum mode

The force to displacement transfer function for the pendulum mode is given by

$$H(w) = \tfrac{1}{m_c} \frac{1}{\left(w_0^2 - w^2\right) + i w_{0w}^2\, j\,(w)}$$

[14]

where ω_{0w} is given by

$$w_{0w}^2 \equiv \frac{k_{el}}{m} = \frac{\dfrac{4 \cdot 2 \cdot \sqrt{\Lambda E I_2}}{2L_w^2}}{m_c}$$

$$\Lambda = \frac{m_c}{4} \cdot g$$

$$I_2 = \frac{p}{4} r_w^4$$

[15]

Λ is the wire tension (we use "4 wires"), the 2 in the numerator is due to having two flexural points.
The ω_0 frequency in equation [14] is given by:

$$w_0^2 = w_{0g}^2 + w_{0w}^2$$
$$w_{0g}^2 = \frac{g}{L_w}$$

[16]

and the loss angle takes into account the residual clamp losses and the thermoelastic effect [Ref: 6]:

$$j(w) = j_w + j_e + j_{te}(w) = j_w + j_e + \Delta \frac{w t}{1+(w t)^2}$$
$$\Delta = \frac{E a_{st}^2 T}{c_{st}} \qquad t = \frac{c_{st}(2r_w)^2}{2.16 \cdot 2p \cdot k_{st}}$$
$$j_w + j_e + j_{te}(2p \cdot 0.6) = \frac{D_F^{-1}}{Q_{meas}} = \frac{\left\{\frac{1}{L_w}\sqrt{\frac{4E I_2}{m_c g}}\right\}^{-1}}{8 \cdot 10^5}$$

[17]

Using the Fluctuation-Dissipation theorem, the fluctuation spectrum is obtained:

$$\langle x(w)\rangle^2 = \frac{4k_b T}{w} \cdot \mathrm{Im}\{H(w)\} = \frac{4k_b T}{w} \cdot \left[m_c w_{0w}^2 j(w)\right] \cdot |H(w)|^2$$

[18]

and the equivalent h is

$$h_{Pend}(f) = \frac{2}{L_{arm}}\sqrt{\langle x(w)\rangle^2}$$

[19]

Vertical oscillation

The force to displacement transfer function for the vertical mode is

$$H_{vt}(w) = \frac{1}{m_c} \frac{1}{(w_{vt}^2 - w^2) + i w_{vt}^2 j(w)}$$
$$w_{vt}^2 = \frac{\frac{p r_w^2 E}{L_w}}{\frac{m_c}{4}}$$

[20]

The displacement spectrum is

$$\langle y(w)\rangle^2 = \frac{4k_b T}{w} \cdot \mathrm{Im}\{H_{vt}(w)\} = \frac{4k_b T}{w} \cdot \left[m_c w_{vt}^2 j(w)\right] \cdot |H_{vt}(w)|^2$$

[21]

and the equivalent h is

$$h_{vt}(f) = \frac{2q_0}{L_{arm}}\sqrt{\langle y(w)\rangle^2}$$

[22]

Violin modes

The violin modes contribution can be derived by [Ref: 7]. The displacement spectrum expression is

$$\langle x_{viol}(w)\rangle^2 = 4\cdot\frac{4k_BT}{w}\,\frac{2r_w r_w^2}{p\cdot m^2}\,L\sum_n \frac{1}{n^2}\,\frac{w_n^2\cdot j_n}{\left(w_n^2 - w^2\right)^2 + \left(w_n^2\cdot j_n\right)^2}$$

$$\frac{w_n}{2p} = \frac{n}{2L_w}\cdot\sqrt{\frac{\frac{m_c g}{4}}{pr_w^2\cdot r_w}}\cdot\left[1 + \frac{2}{L_w}\sqrt{\frac{E\cdot I_2}{\frac{m_c g}{4}}}\right]$$

$$j_n = \frac{2j(w_n)}{L_w}\sqrt{\frac{E\cdot I_2}{\frac{m_c g}{4}}}\cdot\left\{1 + \frac{(n\cdot j(w_n))^2}{2L_w}\cdot\sqrt{\frac{E\cdot I_2}{\frac{m_c g}{4}}}\right\}^{-1}$$

[23]

and the equivalent h is

$$h_{viol}(f) = \frac{2}{L_{arm}}\sqrt{\langle x_{viol}(w)\rangle^2}$$

[24]

Tilt mode and rotational mode

Other two pendulum oscillations must be analysed, the tilt mode (mirror oscillation around a horizontal axis perpendicular to the laser beam), and the rotational mode (mirror oscillation around a vertical axis). The expression that defines the angular displacement is similar to equation [18], where the appropriate angular frequency must be used. Those modes have no effect on the first order angle on the VIRGO sensitivity because the optical path difference is $\delta L \approx L\cdot\theta^2$.

Test mass thermal noise

The test mass internal vibration mode contribution to the sensitivity of a GW interferometric detector like VIRGO has been investigated in several articles (see [Ref: 3, Ref: 12, Ref: 13, Ref: 14 and Ref: 15]). The PSD of the fluctuation is given by the usual F-D theorem expression:

$$\langle \tilde{x}(w)\rangle^2 = \frac{4k_bT}{w^2}\cdot \mathrm{Re}\left(\frac{1}{Z(w)}\right)$$

[25]

where $Z(\omega)$ is the mechanical impedance of the system. Two different methods are used to calculate the equation [25]:

1. Expansion of the vibrating state of the mirror on a basis of normal modes

$$\langle \tilde{x}(w)\rangle^2 = \frac{4k_bT}{w}\cdot\sum_n \frac{j_n(w)}{M_n^{eff} w_n^2} \approx \frac{4k_bT}{w}\cdot j_{quartz}\cdot\sum_n \frac{1}{M_n^{eff} w_n^2}$$

[26]

2. Static deformation of the mirror under a gaussian pressure (Ref: 13, Ref: 14 and Ref: 15)

$$\left\langle \tilde{x}_{low}(w) \right\rangle^2 = \frac{8k_b T}{w} \cdot j\,(w)\{U_0 + \Delta U\}$$

[27]

We used a combination of the two methods because of we need to describe the behaviour of the mirror at low frequency and in the neighbouring of the resonance. The only resonance taken in account is the mode (011 @ ~5600Hz) because of if the beam is well centered, it is the only one directly visible in the Virgo frequency range. For each frequency we used as thermal noise value the largest number between those given by the equation [27] (using formulas in Ref: 15 with the physical parameters reported in this note) and the first mode:

$$\left\langle \tilde{x}_{m_1}(w) \right\rangle^2 = \frac{4k_b T}{w} \cdot \frac{j_{quartz} \cdot w_1^2}{M_1^{eff}\left[\left(w_1^2 - w^2\right)^2 + \left(j_{quartz} \cdot w_1^2\right)^2\right]}$$

[28]

Using the geometrical and structural characteristics of the VIRGO mirrors, we have:

$$w_1^{Near} \approx 2p \cdot 5640 \qquad w_1^{Far} \approx 2p \cdot 5582$$

$$M_1^{eff}\Big|^{Near} \approx 6.57 \qquad M_1^{eff}\Big|^{Far} \approx 6.48$$

$$h_{Mirror}(f) = \frac{\sqrt{2}}{L_{arm}} \sqrt{\sum_{Near,Far} \max\left\{ \left\langle \tilde{x}_{low}(2p\ f) \right\rangle^2, \left\langle \tilde{x}_{m_1}(2p\ f) \right\rangle^2 \right\}}$$

[29]

Thermodynamical noise in the mirrors

Braginsky and collaborators (Ref: 16) showed that the themperature fluctuation in the mirror are coupled to the motion of the reflecting surface through the thermal expansion coefficient in the bulk and through the thermall refractive index in the coating. All the formulas reported are extracted or derived from Ref: 15.

Thermodynamical fluctuation in the bulk:

The amplitude spectral density, in therms of 1/sqrt(Hz), is

$$h_{Brag}(f) = \frac{1}{L_{arm}} \frac{2\sqrt{2k_b k_{FS}}\,T a_{FS}\left(1 + s_{FS}\right)}{p^{\frac{5}{4}} c_{FS}\, r_{FS}} \frac{1}{f} \sqrt{\frac{2}{wN^3} + \frac{2}{wF^3}} \approx 8 \cdot 10^{-24} \left[\frac{10Hz}{f}\right]$$

[30]

Thermodynamical fluctuation in the coating:

The amplitude spectral density, in therms of 1/sqrt(Hz), is

$$h_{Brag}(f) = \frac{1}{L_{arm}} \frac{l}{4p} \frac{d\Phi}{dn} \frac{dn}{dT} \frac{2\sqrt{2k_b}\,T}{\left(p k_{FS} c_{FS}\, r_{FS}\right)^{\frac{1}{4}}} \frac{1}{f^{\frac{1}{4}}} \sqrt{\frac{2}{wN^2} + \frac{2}{wF^2}} \approx 2 \cdot 10^{-24} \left[\frac{10Hz}{f}\right]^{\frac{1}{4}}$$

[31]

where it has been used:

$$\frac{d\Phi}{dn} = 2.8 \qquad \frac{dn}{dT} = 1.5 \cdot 10^{-5}$$

[32]

Mechanical Shot Noise (Creep)

Anelastic relaxation (creep) of the last stage suspension wires can cause a sort of shot noise that can be interpreted as a signal. The complete analysis of this effect is reported in [Ref: 8]. The result is dominated by two parameters, the creep event size q_s, the creep rate λ_s, and by the filter effect caused by the pendulum itself. Experimental measurement of the integral lengthening determines the value of the product $\lambda_s \cdot q_s$ and measurement of the creep PSD gives the product $\lambda_s \cdot \sqrt{q_s}$. The equivalent h is

$$h_{creep}(f) = \frac{q_0}{2L_{arm}} \frac{q_s \sqrt{l_s}}{2p\ f} \cdot m_c w_{vt}^2 \cdot \left| H_{vt}(2p\ f) \right|$$

$$q_s = 10^{-15} \qquad l_s = 20$$

[33]

Viscous damping processes in the pendulum mode

Equation [18] has been calculated using a structural damping model for the pendulum mode. In addition, some process can introduce some viscous contribution to the equation.

Reference mass eddy currents

In [Ref: 9] it has been shown that reference mass eddy currents induced by the mirror magnets can limit the pendulum Q at $Q_{Eddy}=6.1 \cdot 10^7$ for a typical VIRGO suspension. This contribution is viscous because it depends on the mirror-reference mass relative speed.

Residual gas limiting Q

The residual molecules of gas (hydrogen) can limit the maximum Q reachable by the pendulum. This is a typical viscous damping effect and the Q limit is given by

$$Q_{gas} = 4 \frac{m_c}{pr^2} \frac{w_0}{P_T} \sqrt{\frac{p\, k_b T}{8m_{H_2}}}$$

[34]

where μ_{H2} is the mass of the H_2 molecule.
All the viscous damping effects modify equation [18] through a modification in equation [14]:

$$H(w) = \frac{1}{m_c} \frac{1}{\left(w_0^2 - w^2\right) + i\left[w_{0w}^2 j(w) + w \cdot w_{0g} \cdot \left(\frac{1}{Q_{Eddy}} + \frac{1}{Q_{gas}}\right)\right]}$$

[35]

and equation [18] become:

$$\left\langle x(w) \right\rangle^2 = \frac{4k_b T}{w} \cdot \mathrm{Im}\{H(w)\} = \frac{4k_b T}{w} \cdot \left\{ m_c \left[w_{0w}^2 j(w) + w \cdot w_{0g} \cdot \left(\frac{1}{Q_{Eddy}} + \frac{1}{Q_{gas}} \right) \right] \right\} \cdot \left| H(w) \right|^2$$

[36]

Low pressure acoustic noise

In VIRGO lower tower, the vibration of external walls can be transmitted to the mirror through the residual gas molecules. This effect is analysed in [Ref: 11].
The resulting h is

$$h_{Acoustic}(f) = \frac{2}{L_{arm}} \frac{\frac{k_b T}{P_T}}{2p^{3/2}} \cdot \frac{p\ R_c^2}{m_c f} \cdot \tilde{x}_{seim}(f)$$

[37]

If we use the VIRGO numbers results $h_{Acoustic}(f) \approx 2 \cdot 10^{-24}/f^3$.

Non-linear opto-thermal coupling

Laser power fluctuation can couple to the absorption asymmetry (α_1-α_2) in the two Fabry-Perot cavities in VIRGO. This effect has been investigated in [Ref: 10, Ref: 1].
The result is summarised in the following formulae:

$$h_{\Delta a}(f) = \frac{h_c}{2L_{arm}} \frac{dn}{dT} \cdot (a_1 - a_2) \cdot \tilde{T}(f)$$

$$\tilde{T}(f) \approx 7.7 \cdot 10^{-5} \cdot \frac{d\tilde{P}(f)}{f}$$

$$\frac{d\tilde{P}(f)}{P} = \frac{3.1 \cdot 10^{-6}}{f^{1.5}} + 1.82 \cdot 10^{-9} + 8.18 \cdot 10^{-17} \cdot f^2$$

$$a_1 - a_2 \approx 0.2 \quad \frac{ppm}{cm}$$

$$h_{\Delta a}(10) \approx 1.5 \cdot 10^{-24}\, Hz^{-\frac{1}{2}}$$

[38]

Distorsion by laser heating

Laser heating can cause displacement noise via the thermal expansion coefficient (Ref: 15). The distortion of the reflecting surface affects the thermal noise amplitude through the relation:

$$x(f) = \Theta \frac{P(f)}{f} = \frac{a_{FS}(1 + s_{FS})e}{r_{FS} c_{FS} p^2 w^2} \frac{P(f)}{f}$$

[39]

where ε~1ppm. The first contribution to the power fluctuation *P(f)* is due to the shot noise:

$$h_{dist}(f) = \frac{1}{L_{arm}} \frac{\sqrt{2P_{cavity} \frac{hc}{l}}}{f} \sqrt{2\Theta_N^2 + 2\Theta_F^2}$$

[40]

The second contribution is due to the laser power fluctuation, but it requires a certain Finesse asymmetry ΔF between the two Fabry-Perot cavities:

$$h_{dist}(f) \approx \frac{1}{L_{arm}} \frac{\Delta F}{F} C \cdot \frac{2F}{p} \frac{d\tilde{P}(f)}{f} \sqrt{2\Theta_N^2 + 2\Theta_F^2}$$

[41]

where h(10Hz)~$1.6 \cdot 10^{-25}$.

Phase reflectivity of the coating

The temperature fluctuation causes also the modulation of the refraction index of the dielectric layers stack of the coating (Ref: 15). The equivalent spectral amplitude is

$$h_{refl}(f)=\frac{l\,\frac{d\Phi}{dn}\frac{dn}{dT}e}{p\sqrt{pr_{FS}c_{FS}k_{FS}}}\frac{1}{\sqrt{2wN^{4}+2wF^{4}}}\frac{1}{\sqrt{f}}P(f)$$

[42]

where

$$P(f)=\sqrt{2P_{cavity}\frac{hc}{l}}$$

[43]

if the responsible for power fluctuation is the shot noise, and

$$P(f)=\frac{\Delta F}{F}P_{cavity}\frac{d\tilde{P}(f)}{P}$$

[44]

if the responsible for power fluctuation is the laser unstability coupled to the Finesse asymmetry. In the first case we obtain $h(f)\sim 4\cdot 10^{-28}\cdot(1/f)^{1/2}$; in the second case is $h(10Hz)\sim 2.7\cdot 10^{-26}$.

Residual gas pressure fluctuation

The fluctuation of the residual gas in the VIRGO vacuum pipe can cause a laser beam phase fluctuation because of the relation existing between the refraction index and the residual gas pressure value:

$$n=1+e_{H_2}\frac{P_{tube}}{P_{atm}} \quad\rightarrow\quad dn=e_{H_2}\frac{dP_{tube}}{P_{atm}}=e_{H_2}\frac{dN_{tube}}{N_{atm}}$$

[45]

where N_{tube} and N_{atm} are the molecule densities and

$$e_{H_2}\approx 1.2\cdot 10^{-4}$$

[46]

The h equivalent given by pressure fluctuations is:

$$h_{dP}=\frac{e_{H_2}}{N_{atm}}\sqrt{\frac{W_{beam}}{v_{H_2}}\cdot\frac{N_{tube}}{V_{beam}}\sqrt{p}}\approx 2.5\cdot 10^{-26}$$

[47]

where W_{beam} is the beam waist at the far mirror distance (≈0.1m), v_{H2} is the H_2 molecule velocity and V_{beam} is the "volume" of the beam ($\pi\cdot W_{beam}^{2}\cdot L_{arm}$).

Conclusions

The overall results are plotted in figure 1 where all the described contributions are reported.

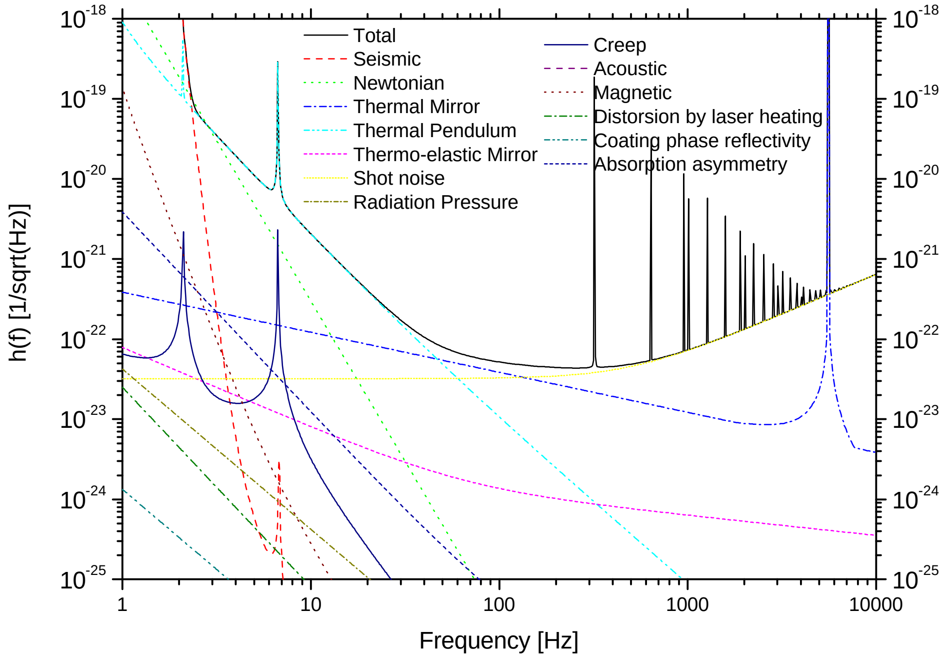

Figure 1 - Virgo Sensitivity curve

References

Ref: 1 The VIRGO **D**ata **A**nalysis **D**ocument, VIR-TRE-DIR-7000-109 (24/05/1999)

Ref: 2 G.Cella, E.Cuoco et al., *Classical and Quantum Gravity* 15, p.1-24 (1998)

Ref: 3 P.R. Saulson, Phys. *Rev. D 30 (4)* 732-736 (1984)

Ref: 4 P.R. Saulson, *Fundamentals of Interferometric Gravitational Wave Detectors*, World Scientific Pub Co; ISBN: 9810218206 (1994)

Ref: 5 B.J. Meers, *Phys. Rev. D 38 (8)* 2317-2326 (1988)

Ref: 6 G.Cagnoli et al. *Phys. Lett. A, 255*, 230-235 (1999)

Ref: 7 P.R. Saulson, *Phys. Rev. D 42* (8) 2437-2445 (1990)

Ref: 8 C.Cagnoli et al., *Phys. Lett. A, 237*, (1-2), 21-27 (1998)

Ref: 9 C.Cagnoli et al., *Rev. Sci. Instrum. 69* (7) 2777-2780 (1998)

Ref: 10 P.Hello and J.Y.Vinet, *Phys.Lett. A 230*, 12-18 (1997)

Ref: 11 F.Barone et al. VIR-NOT-NAP-1390-053 (1996)

Ref: 12 F.Bondu and J.Y.Vinet, *Phys Lett. A 198*, 74 (1995)

Ref: 13 F.Bondu et al., VIR-NOT-LAS-1390-108 (1998)

Ref: 14 Y.Levin, *Phys. Rev. D 57 (2),* 659-663 (1998)

Ref: 15 J.Y.Vinet, VIR-LAS 10/2000 (Oct.2000)

Ref: 16 V.B.Braginsky et al., *Phys Lett.A* 264, 1-10, (1999)

Ref: 17 F. Bondu., *Virgo internal Note, VIR-NOT-OCA-1390-243 (2003)*